Journal of Materials Chemistry C

ROYAL SOCIETY OF CHEMISTRY

PAPER

View Article Online
View Journal | View Issue

Cite this: J. Mater. Chem. C, 2021, 9, 4200

Tyrian purple: an ancient natural dye for cross-conjugated n-type charge transport†

Kealan J. Fallon,[a] Nilushi Wijeyasinghe,[b] Anastasia Leventis,[a] Jose M. Marin-Beloqui,[c] Daniel T. W. Toolan,[d] Mohammed Al-Hashimi,[e] Tracey M. Clarke,[c] Thomas D. Anthopoulos[b] and Hugo Bronstein *[a]

Received 25th November 2020,
Accepted 18th December 2020

DOI: 10.1039/d0tc05553k

rsc.li/materials-c

Herein, we present two novel organic semiconducting polymers synthesised from an ancient dye. By employing cross-conjugation within the polymer backbone as a synthetic strategy, we are able to engineer optical gaps such that the novel materials absorb over the entire visible spectrum. The cross-conjugated polymers exhibited relatively high n-type charge transport performance in organic field-effect transistors, a rare characteristic for this type of polymer. Quantum chemical calculations provide insight into this behaviour, suggesting that, whilst conjugation along the HOMO is indeed inhibited *via* molecular design, these materials possess highly delocalized LUMOs, facilitating high n-type charge transport.

Introduction

Organic semiconducting polymers have received large attention in the past two decades due to their low cost, mechanical flexibility, and ease of processing. Their effectiveness as donor materials in the bulk heterojunction of organic photovoltaics (OPVs) and in transporting charge carriers in organic field-effect transistors (OFETs) is reliant on the energetic tailoring of frontier molecular orbital (MO) energy levels and thus the band gap between them. The most widely employed strategy for band gap engineering is in alternating donor–acceptor (D–A) copolymers, where the energy of the highest occupied molecular orbital (HOMO) is typically dictated by the donor unit whilst the energy of the lowest unoccupied molecular orbital (LUMO) is dictated by the acceptor.[1–3]

A design approach which has seldom been investigated is the interruption of conjugation along a polymer backbone. Due to their shorter effective conjugation lengths, cross-conjugated polymers typically have wider band gaps and increased ionisation potentials, making them more stable to oxidative doping when operated in air.[4,5] Heeney *et al.* demonstrated the first successful use of a thieno[2,3-*b*]thiophene cross-conjugated polymer as a p-type OFET material, exhibiting hole transport up to 0.05 $cm^2\ V^{-1}\ s^{-1}$.[6] Recently, Zhang *et al.* reported high hole mobilities in diketopyrrolopyrrole (DPP) based cross-conjugated polymers.[7] Other common building blocks have been exploited in cross-conjugated polymers including isoindigo,[8,9] fluorene,[10–13] carbazole,[14] and some more atypical systems,[15–20] however successful application in devices is rarely reported.

Our recent work on conjugated organic polymers exploiting the relatively unexplored building block indolonaphthyridine (IND) was inspired by the chromophore of natural indigo dye. These materials with fully conjugated non-planar backbones exhibited narrow optical band gaps (~1.2 eV), gave high power conversion efficiencies in OPVs (up to 4.1%), and gave high performance charge transport in OFETs for holes and electrons up to 1.0 and 3.1 $cm^2\ V^{-1}\ s^{-1}$ respectively.[21]

INDs are formed through a dual condensation-annulation reaction of indigo and an aromatic acetyl chloride. The benzene rings of the indigo dye are not involved in the conjugation of the IND unit and offer the potential to introduce cross-conjugation. Tyrian Purple (6,6′-dibromoindigo, **5**) is a naturally occurring dye of significant legacy. The precursors of the dye were historically extracted from the sea snail *Murex brandaris*, which underwent oxidative coupling in air to form the brilliantly purple solid. A ghastly 8500 snails were required to harvest 1 g of the dye, leading to the high wealth associated with the colour purple throughout history until cheaper synthetic alternatives were discovered in the late 1800s.[22] Fatefully, it cannot be simply

[a] Department of Chemistry & Physics, University of Cambridge, Lensfield Road, Cambridge, CB2 1EW, UK. E-mail: hab60@cam.ac.uk
[b] King Abdullah University of Science and Technology, KAUST Solar Center, Thuwal 23955-6900, Saudi Arabia
[c] Department of Chemistry, University College London (UCL), London WC1H 0AJ, UK
[d] Department of Chemistry, University of Sheffield, Dainton Building, Brook Hill, Sheffield S3 7HF, UK
[e] Department of Chemistry, Texas A&M University at Qatar, P. O. Box 23874, Doha, Qatar

† Electronic supplementary information (ESI) available. See DOI: 10.1039/d0tc05553k

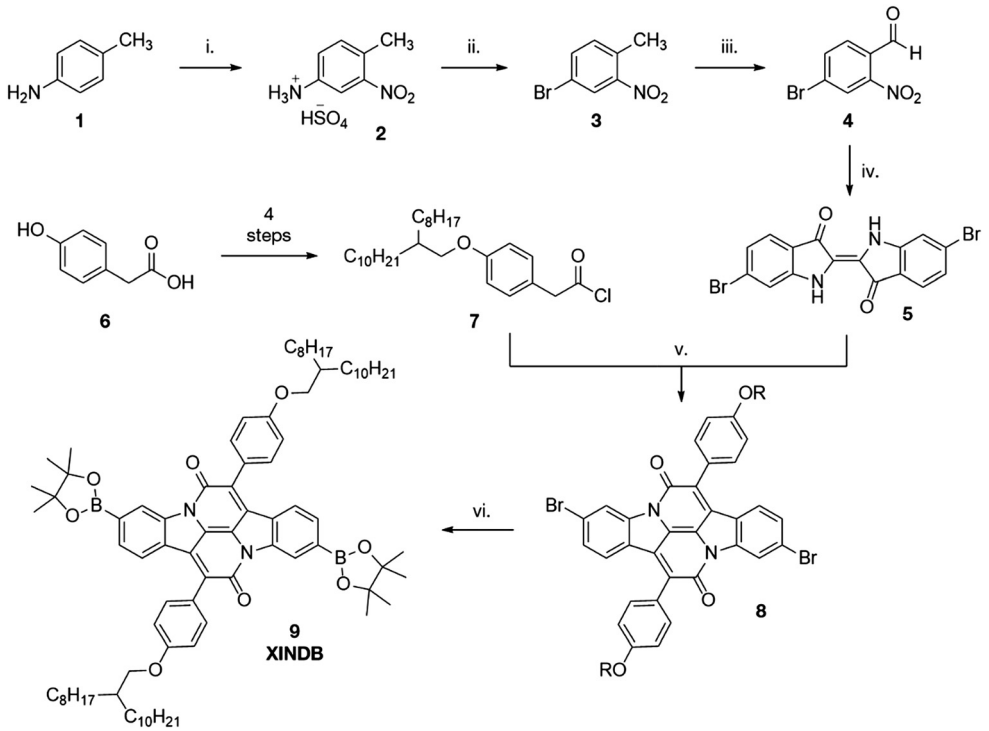

Scheme 1 Synthesis of monomer (i) HNO_3, H_2SO_4, 83% (ii) $NaNO_2$, HBr, CuBr, 57% (iii) DMF·DMA then $NaIO_4$, 67% (iv) NaOH, $(CH_3)_2CO$, 58% (v) xylenes, Δ, 6%, R = 2-octyldodecanyl (vi) $PdCl_2$(dppf), B_2pin_2, dioxane, 87%.

prepared by the bromination of indigo, which results in bromination of all positions except the 6-position.[23] Whilst several preparations have been reported, none are particularly high yielding.[24,25] Herein we report a facile, high-yielding four-step synthesis (Scheme 1), adapted from Imming *et al.*[26]

Results and discussion

Following nitration of 4-methylphenylammonium hydrosulfate, a Sandmeyer reaction yields the desired brominated nitrotoluene **3**. Oxidation of the methyl group using DMF·DMA and $NaIO_4$ provides the desired aldehyde **4** in high yield. Tyrian purple **5** was then synthesised from this aldehyde through a straightforward Baeyer–Drewson indigo synthesis in good yield. Condensation of **5** with acetyl chloride **7** gave the brominated indolonaphthyridine benzene **8**, which underwent a high yielding Miyaura borylation to give the diborylated cross-conjugated monomer **XINDB** (**9**).

This monomer subsequently underwent a high yielding Suzuki co-polymerisation of **9** with dibrominated DPPT[27] and INDT monomers to give the cross-conjugated polymers **XINDB–DPPT** (**P1**) and **XINDB–INDT** (**P2**) in high yield (Fig. 1), which both exhibited excellent solubility in typical organic solvents.

The polymers were purified by Soxhlet extraction first with acetone then hexane, to remove impurities and low molecular weight oligomers, then finally chloroform. The physical properties of the polymers are shown in Table 1. Molecular weights were determined by size exclusion chromatography (SEC) using polystyrene (PS) standards eluting with chlorobenzene at 80 °C. The DPP-containing polymer **P1** exhibited very high molecular weight, whilst the INDT-containing polymer **P2** exhibited relatively lower molecular weight averages.

Fig. 2 shows the UV-vis absorption spectrum of the brominated monomer and the two polymers. Both cross-conjugated polymers exhibited broad absorption in the visible and near-IR regions. The optical band gaps (E_g) of the polymers were estimated from the absorption onsets of 805 nm for **P1** and 865 nm for **P2**, indicating E_g of 1.54 and 1.43 eV respectively. These band gaps are notably wider than typical DPP and INDT conjugated polymers, ratifying the strategy of cross-conjugated design to widen the optical gap. Both absorptions exhibited a bathochromic shift in thin-film, attributed to solid-state packing effects. The ionisation potential (E_{HOMO}) of the two polymers were measured using photoelectron spectroscopy in air (PESA) and the electron affinities (E_{LUMO}) were estimated by the addition of the respective optical band gap to the measured ionisation potential. In our previous work, all conjugated IND-based polymers exhibited isoenergetic electron affinities of approximately −3.75 eV, irrespective of co-monomer (benzene, thiophene, selenophone, benzothiadiazole). Interestingly, E_{LUMO} of **P1** and **P2** were −3.75 and −3.78 eV respectively, fitting this trend, demonstrating the remarkable ability of the electron deficient indolonaphthyridine building block at controlling E_{LUMO}. The widening of the optical band gap seen in these cross-conjugated polymers results from a deeper E_{HOMO} of −5.29 and −5.21 eV for **P1** and **P2** respectively.

Theoretical analysis of the electronic structure of the two polymers was carried out on model trimers using the B3LYP

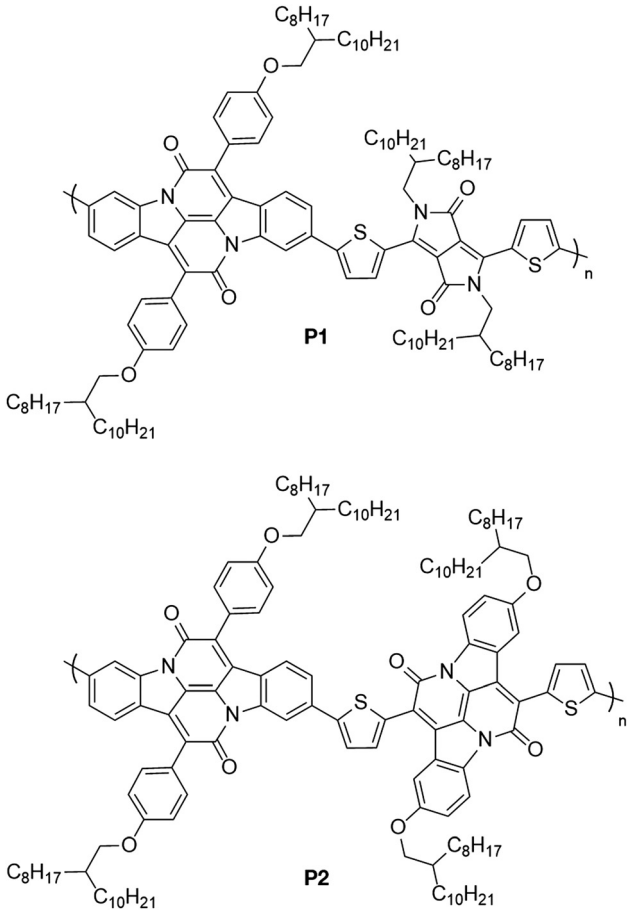

Fig. 1 Structures of the two polymers in this study.

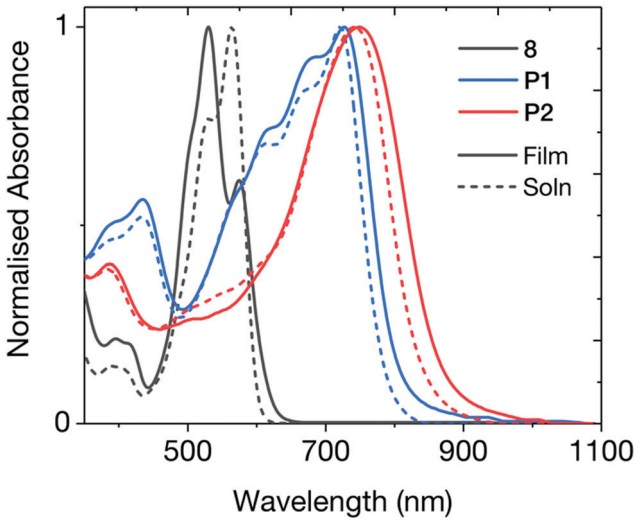

Fig. 2 Normalized UV-vis absorption spectra of the two cross-conjugated polymers and the dibrominated indolonaphthyridine. Solution spectra were recorded in chlorobenzene, and thin-films were spun from 5 mg mL^{-1} solutions in chlorobenzene.

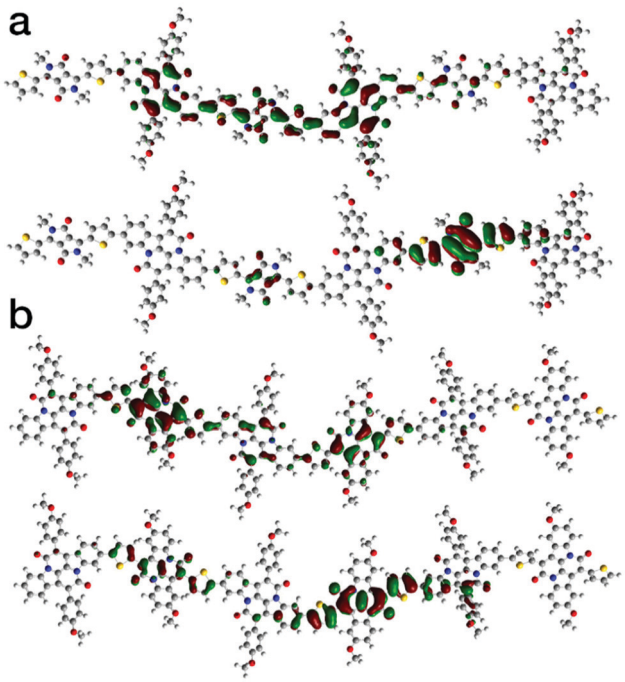

Fig. 3 Theoretical distributions of the LUMO (top) and HOMO (bottom) of (a) **P1** and (b) **P2** calculated at B3LYP/6-31G*.

hybrid functional and the 6-31G* basis set.[28] The calculated frontier molecular orbital distributions are shown in Fig. 3. Despite the cross-conjugation, the calculations indicate the LUMO of both polymers are delocalised along the polymer backbones. In contrast, the HOMO of both polymers is localised strongly on the DPPT and INDT units. This is in agreement with previous theoretical studies on the electronic structure of indigo-containing polymers.[29]

To investigate the charge transport properties of the two cross-conjugated polymers, unipolar top gate bottom contact (TG-BC) OFET devices were fabricated on glass substrates using thermally evaporated source/drain (SD) electrodes. For n-type operation, Al SD electrodes were treated with ethoxylated polyethylenimine (PEIE) to facilitate electron injection by reducing the work function of the electrodes to better match

Table 1 Physical and optical properties of the two cross-conjugated polymers

Polymer	M_n[a] (kDa)	M_w[a] (kDa)	$Đ$[a]	λ_{max}^{soln}[b] (nm)	λ_{max}^{film}[c] (nm)	HOMO[d] (eV)	LUMO[e] (eV)	E_g (eV)[b]	E_g^{calc}[f] (eV)
P1	84	551	6.6	720	727	−5.29	−3.75	1.54	1.61
P2	11	53	5.0	743	750	−5.21	−3.78	1.43	1.70

[a] Determined by SEC(PS) using PhCl as eluent. [b] PhCl solution. [c] Spin-coated from PhCl 5 mg mL^{-1}. [d] Determined by PESA. [e] HOMO + optical band gap. [f] Determined by TD-DFT using B3LYP/6-31g*.

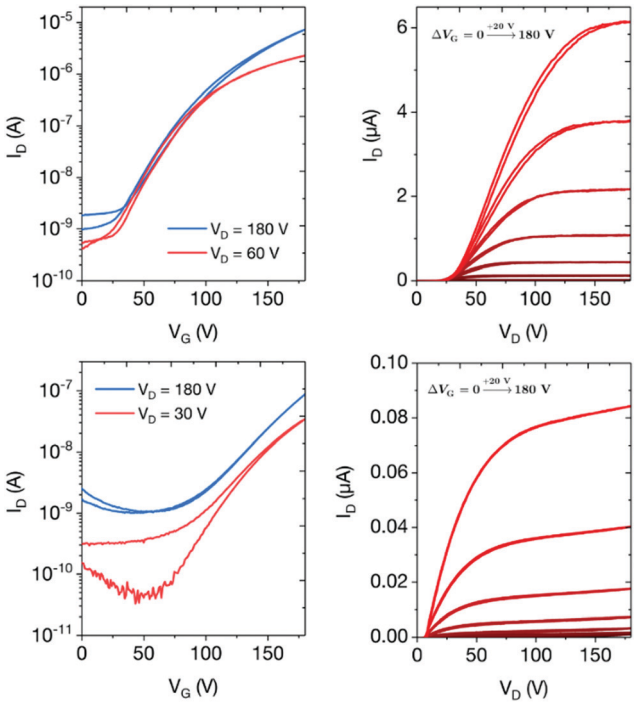

Fig. 4 Transfer curves (left) and output characteristics (right) of n-type TG-BC OFET devices based on **P1** (top) and **P2** (bottom) semiconductor layers annealed at 190 °C, with channel dimensions of L = 40 μm and W = 1000 μm.

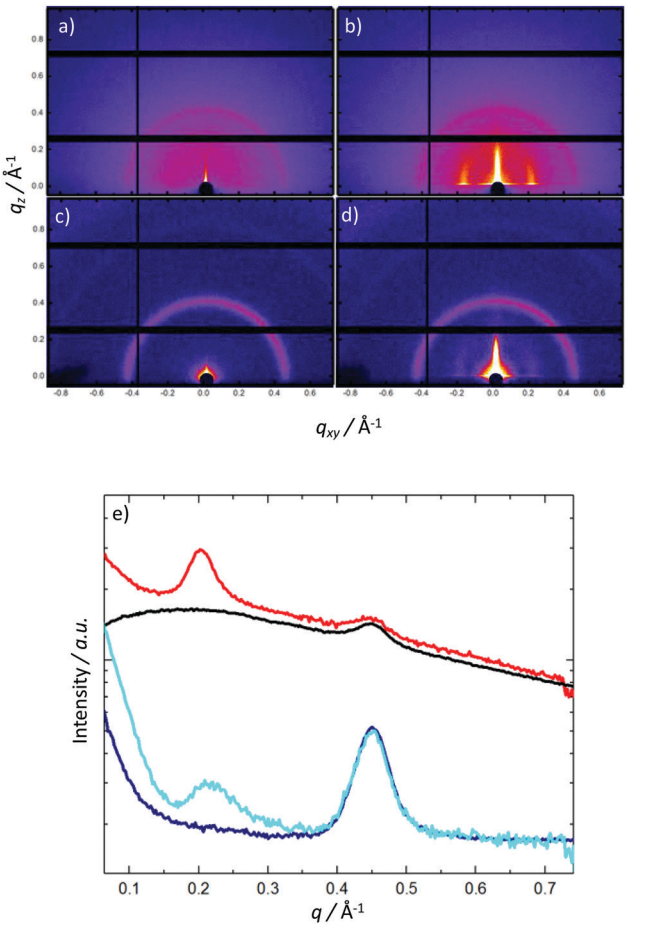

Fig. 5 2D X-ray grazing incidence scattering data, for **P2** [as-cast (a) & annealed (b)] and **P1** [as-cast(c) & annealed (d)], and horizontally integrated X-ray scattering data (e) to highlight the development of in plane scattering features for **P2** [as-cast(black), annealed (red)] and **P1** [as-cast(blue) & annealed (cyan)].

the electron affinities of the polymers. For p-type operation, the treatment of Au electrodes with UV/O_3 removes surface contaminants and is expected to improve the hole injection into polymers with HOMO energies of −5.29 eV (**P1**) and −5.21 eV (**P2**). Kelvin probe contact potential difference measurements verified that the work function of the treated Au surface (5.3 eV) was an excellent match to the HOMO energies of the two polymers. The semiconductor layer was spin-cast onto the SD electrodes from 10 mg mL^{-1} solutions in chlorobenzene, followed by annealing at 190 °C for 15 min. Finally, an amorphous fluoropolymer dielectric (CYTOP) was spin-cast onto the semiconductor and the device further annealed for 1 h at 100 °C. Each device was completed with a thermally evaporated Al gate electrode.

Despite the outlined efforts, the cross-conjugated polymers only exhibited n-type charge transport – no hole transport was observed in the devices designed for p-type operation. These results correspond well with the theoretical molecular orbital distributions and we attribute the lack of hole current primarily to the strongly localized HOMOs on the DPPT and INDT units, which is expected to hinder hole transport, although we note that further work is required to confirm this. In contrast, the clear delocalization of the LUMOs along the polymer backbone correlates well with the good electron transport in the n-type optimized OFETs.

The transfer and output characteristics of the n-type devices are shown in Fig. 4 and the performance data summarised in Table 2. The maximum drain currents measured in OFETs based on **P1** (≈10 μA) were two orders of magnitude higher than the maximum drain currents in OFETs based on **P2** when similar voltages were applied, indicating clearly that **P1** exhibits superior electron transport in comparison to **P2**. Interestingly,

Table 2 Performance parameters of TG-BC n-type OFET devices based on **P1** and **P2** semiconductor layers, with channel length L = 40 μm and width W = 1000 μm

Polymer	I_{on}/I_{off} (lin)	I_{on}/I_{off} (sat)	V_{on}^{lin} (V)	V_{th}^{sat} (V)	$\mu_{lin}{}^a$ (cm^2 V^{-1} s^{-1})	$\mu_{sat}{}^a$ (cm^2 V^{-1} s^{-1})
P1	10^3 to 10^4	10^3 to 10^4	+23	+91	0.012 (0.010)	0.10 (0.09)
P2	10^2	10^2	+41	+123	0.0007 (0.0007)	0.0019 (0.0017)

[a] Field-effect electron mobility extracted from smoothed data, indicating the best of three devices measured and the mean value given in brackets.

considering the almost isoenergetic LUMO energies of the two polymers, this result is supported by the molecular orbital distributions in Fig. 3, which indicate that the LUMO of **P1** exhibits a greater degree of delocalization along the polymer backbone relative to **P2**. The on–off ratios in the linear and saturated regimes for **P1** (10^3 to 10^4) were up to two orders of magnitude higher than **P2** (10^2), again demonstrating the better performance of the DPP-based polymer.

Field-effect electron mobilities for the two polymers were calculated from the transfer characteristics using the standard gradual channel approximation. Due to poor device performance at low V_D, electron mobilities calculated in the linear regime were 0.012 and 0.0007 $cm^2\ V^{-1}\ s^{-1}$ for **P1** and **P2**, respectively. In the saturation regime, the electron mobilities were 0.10 and 0.002 $cm^2\ V^{-1}\ s^{-1}$ for **P1** and **P2** respectively, representing respectable values for these types of materials. Notably, the mobility of **P1** is 17× higher than the most comparable previously reported polymer.[30] Whilst conjugated indolonaphthyridine polymers have exhibited ambipolar charge transport, our results showcase the ability to switch to unipolar characteristics by exploiting cross-conjugation and MO localization as a synthetic design strategy.

To examine the solid state structures of the two polymers, we performed grazing incidence X-ray scattering (Fig. 5). For both the as-cast polymers, only scattering from the glass substrate is observed (q = 0.45 $Å^{-1}$). Thermal annealing results in the development of perpendicular peaks parallel to the substrate at q = 0.20 and 0.217 $Å^{-1}$, corresponding to domain spacings of 31.4 and 29.0 Å for **P2** and **P1**, respectively. The observed perpendicular alignment of the scattering features indicates preferential molecular ordering perpendicular to the substrate. Additionally AFM was carried out on the two polymers (see ESI†) which showed very similar surface morphologies. The similarities in solid state packing between both **P2** and **P1** suggest that the difference in charge-carrier motilities are due to our proposed electronic effects as opposed to differences in polymer microstructure.

Conclusions

In conclusion, we report the synthesis and characterization of two cross-conjugated polymers derived from Tyrian Purple dye. Using this relatively unexplored design strategy, the polymers exhibited notably wider optical gaps compared to previously reported conjugated polymers. Quantum chemical calculations revealed that, despite their cross-conjugated electronic nature, the polymers remarkably exhibited delocalization of their LUMO wavefunction. This characteristic resulted in electron mobilities in field-effect transistors up to 0.1 $cm^2\ V^{-1}\ s^{-1}$. To the best of our knowledge this is the highest efficiency n-type OFET transport to date in indigo-based cross-conjugated organic polymers. These findings confirm the effectiveness of cross-conjugation as a tool for widening the optical band gap of organic semiconductors and demonstrate the ability of indolonaphthyridine to furnish high performance n-type materials with predictable electron affinities.

Conflicts of interest

There are no conflicts to declare.

Acknowledgements

The authors gratefully acknowledge support for this work from the Qatar National Research Fund project number: NPRP 12S-0304-190227, EU project 679789 – 455 CONTREX and the EPSRC grant EP/S003126/1.

Notes and references

1 K. Müllen and W. Pisula, Donor-Acceptor Polymers, *J. Am. Chem. Soc.*, 2015, **137**(30), 9503–9505.
2 R. S. Kularatne, H. D. Magurudeniya, P. Sista, M. C. Biewer and M. C. Stefan, Donor-Acceptor Semiconducting Polymers for Organic Solar Cells, *J. Polym. Sci., Part A: Polym. Chem.*, 2013, **51**(4), 743–768.
3 Y. Zhao, Y. Guo and Y. Liu, 25th Anniversary Article: Recent Advances in n-Type and Ambipolar Organic Field-Effect Transistors, *Adv. Mater.*, 2013, 5372–5391.
4 E. J. Meijer, C. Detcheverry, P. J. Baesjou, E. Van Veenendaal, D. M. De Leeuw and T. M. Klapwijk, Dopant Density Determination in Disordered Organic Field-Effect Transistors, *J. Appl. Phys.*, 2003, **93**(8), 4831–4835.
5 T. M. Swager and R. H. Grubbs, Synthesis and Properties of a Novel Cross-Conjugated Conductive Polymer Precursor: Poly(3,4-Diisopropylidenecyclobutene), *J. Am. Chem. Soc.*, 1987, **109**(3), 894–896.
6 M. Heeney, C. Bailey, K. Genevicius, M. Shkunov, D. Sparrowe, S. Tierney and I. McCulloch, Stable Polythiophene Semiconductors Incorporating Thieno[2,3-6]Thiophene, *J. Am. Chem. Soc.*, 2005, **127**(4), 1078–1079.
7 W. Zhang, Z. Mao, N. Zheng, J. Zou, L. Wang, C. Wei, J. Huang, D. Gao and G. Yu, Highly Planar Cross-Conjugated Alternating Polymers with Multiple Conformational Locks: Synthesis, Characterization and Their Field-Effect Properties, *J. Mater. Chem. C*, 2016, **4**(39), 9266–9275.
8 G. W. P. Van Pruissen, J. Brebels, K. H. Hendriks, M. M. Wienk and R. A. J. Janssen, Effects of Cross-Conjugation on the Optical Absorption and Frontier Orbital Levels of Donor-Acceptor Polymers, *Macromolecules*, 2015, **48**(8), 2435–2443.
9 A. Ganguly, J. Zhu and T. L. Kelly, Effect of Cross-Conjugation on Derivatives of Benzoisoindigo, an Isoindigo Analogue with an Extended π-System, *J. Phys. Chem. C*, 2017, **121**(17), 9110–9119.
10 T. P. Voortman, D. Bartesaghi, L. J. A. Koster and R. C. Chiechi, Cross-Conjugated n-Dopable Aromatic Polyketone, *Macromolecules*, 2015, **48**(19), 7007–7014.
11 S. Romero-Servin, L. A. Lozano-Hernández, J. L. Maldonado, R. Carriles, G. Ramos-Ortíz, E. Pérez-Gutiérrez, U. Scherf

and M. G. Zolotukhin, Light Emission Properties of a Cross-Conjugated Fluorene Polymer: Demonstration of Its Use in Electro-Luminescence and Lasing Devices, *Polymers*, 2016, **8**(2), 43.

12 L. Aparicio-Ixta, G. Ramos-Ortiz, J. L. Pichardo-Molina, J. L. Maldonado, M. Rodríguez, V. M. Tellez-Lopez, D. Martinez-Fong, M. G. Zolotukhin, S. Fomine and M. A. Meneses-Nava, *et al.*, Two-Photon Excited Fluorescence of Silica Nanoparticles Loaded with a Fluorene-Based Monomer and Its Cross-Conjugated Polymer: Their Application to Cell Imaging, *Nanoscale*, 2012, **4**(24), 7751–7759.

13 T. P. Voortman, H. D. De Gier, R. W. A. Havenith and R. C. Chiechi, Stabilizing Cations in the Backbones of Conjugated Polymers, *J. Mater. Chem. C*, 2014, **2**(17), 3407–3415.

14 X. Li, X. Zhang, W. Li, Y. Wang, T. Liu, B. Zhang and W. Yang, Synthesis and Enhanced Two-Photon Absorption Properties of Tetradonor-Containing Anthracene-Centered 2-D Cross-Conjugated Polymers, *J. Mater. Chem.*, 2011, **21**(11), 3916–3924.

15 T. Maeda, T. Tsukamoto, A. Seto, S. Yagi and H. Nakazumi, Synthesis and Characterization of Squaraine- Based Conjugated Polymers with Phenylene Linkers for Bulk Heterojunction Solar Cells, *Macromol. Chem. Phys.*, 2012, **213**(24), 2590–2597.

16 L. V. Kayser, E. M. Hartigan and B. A. Arndtsen, Multicomponent Coupling Approach to Cross-Conjugated Polymers from Vanillin-Based Monomers, *ACS Sustainable Chem. Eng.*, 2016, **4**(12), 6263–6267.

17 S. Barik and S. Valiyaveettil, Synthesis and Self-Assembly of Polyhydroxylated and Electropolymerizable Block Copolymers, *J. Polym. Sci., Part A: Polym. Chem.*, 2014, **52**(15), 2217–2227.

18 E. Preis and U. Scherf, Poly(Diindenonaphthalene) and Poly(Indenofluorene) – Tuning the Absorption Properties of Low Bandgap Cross-Conjugated Polymers, *Macromol. Rapid Commun.*, 2006, **27**(14), 1105–1109.

19 H. Wang, R. Helgeson, B. Ma and F. Wudl, Synthesis and Optical Properties of Cross-Conjugated Bis(Dimethylaminophenyl) Pyridylvinylene Derivatives, *J. Org. Chem.*, 2000, **65**(18), 5862–5867.

20 Q. Fang and T. Yamamoto, Preparation of a New Polymer Containing Photoluminescent Pyrazoline Unit in the Main Chain, *J. Polym. Sci., Part A: Polym. Chem.*, 2004, **42**(11), 2686–2697.

21 K. J. Fallon, N. Wijeyasinghe, E. F. Manley, S. D. Dimitrov, S. A. Yousaf, R. S. Ashraf, W. Duffy, A. A. Y. Guilbert, D. M. E. Freeman and M. Al-Hashimi, *et al.*, Indolo-Naphthyridine-6,13-Dione Thiophene Building Block for Conjugated Polymer Electronics: Molecular Origin of Ultrahigh n-Type Mobility, *Chem. Mater.*, 2016, **28**(22), 8366–8378.

22 P. Friedländer, Über Den Farbstoff Des Antiken Purpurs Aus Murex Brandaris, *Ber. Dtsch. Chem. Ges.*, 1909, **42**(1), 765–770.

23 P. F. Schatz, Indigo and Tyrian Purple—In Nature and in the Lab, *J. Chem. Educ.*, 2009, **78**(11), 1442.

24 J. L. Wolk and A. A. Frimer, A Simple, Safe and Efficient Synthesis of Tyrian Purple (6,6′-Dibromoindigo), *Molecules*, 2010, **15**(8), 5561–5580.

25 C. J. Cooksey, Tyrian Purple: 6,6′-Dibromoindigo and Related Compounds, *Molecules*, 2001, 736–769.

26 P. Imming, I. Imhof and M. Zentgraf, An Improved Synthetic Procedure for 6,6′-Dibromoindigo (Tyrian Purple), *Synth. Commun.*, 2001, **31**(23), 3721–3727.

27 A. Leventis, J. Royakkers, A. G. Rapidis, N. Goodeal, M. K. Corpinot, J. M. Frost, D. K. Bučar, M. O. Blunt, F. Cacialli and H. Bronstein, Highly Luminescent Encapsulated Narrow Bandgap Polymers Based on Diketopyrrolopyrrole, *J. Am. Chem. Soc.*, 2018, **140**(5), 1622–1626.

28 D. M. E. Freeman, A. J. Musser, J. M. Frost, H. L. Stern, A. K. Forster, K. J. Fallon, A. G. Rapidis, F. Cacialli, I. McCulloch and T. M. Clarke, *et al.*, Synthesis and Exciton Dynamics of Donor-Orthogonal Acceptor Conjugated Polymers: Reducing the Singlet-Triplet Energy Gap, *J. Am. Chem. Soc.*, 2017, **139**(32), 11073–11080.

29 C. Guo, J. Quinn, B. Sun and Y. Li, Regioisomeric Control of Charge Transport Polarity for Indigo-Based Polymers, *Polym. Chem.*, 2015, **6**(39), 6998–7004.

30 C. Guo, J. Quinn, B. Sun and Y. Li, An Indigo-Based Polymer Bearing Thermocleavable Side Chains for n-Type Organic Thin Film Transistors, *J. Mater. Chem. C*, 2015, **3**(20), 5226–5232.